Phase switching in population cycles

Shandelle M. Henson[1]*, J. M. Cushing[2], R. F. Costantino[3], Brian Dennis[4] and Robert A. Desharnais[5]

[1]Department of Mathematics, [2]Interdisciplinary Program in Applied Mathematics, University of Arizona, Tucson, AZ 85721, USA (henson@math.arizona.edu, cushing@math.arizona.edu)
[3]Department of Biological Sciences, University of Rhode Island, Kingston, RI 02881, USA (byg101@uriacc.uri.edu)
[4]Department of Fish and Wildlife Resources and Division of Statistics, University of Idaho, Moscow, ID 83844, USA (brian@uidaho.edu)
[5]Department of Biology and Microbiology, California State University, Los Angeles, CA 90032, USA (rdeshar@calstatela.edu)

Oscillatory populations may exhibit a phase change in which, for example, a high–low periodic pattern switches to a low–high pattern. We propose that phase shifts correspond to stochastic jumps between basins of attraction in an appropriate phase space which associates the different phases of a periodic cycle with distinct attractors. This mechanism accounts for two-cycle phase shifts and the occurrence of asynchronous replicates in experimental cultures of *Tribolium*.

Keywords: periodic time-series; stochasticity; phase switching; basins of attraction; nonlinear population dynamics; *Tribolium*

1. INTRODUCTION

Many biological populations, when carefully studied in the laboratory, display temporal cycling in numbers (Hassell & May 1990). Examples include paramecia (Gause 1964), blow flies (Nicholson 1957), bean weevils (Utida 1957), and flour beetles. Indeed, most continuously cultured laboratory populations of the flour beetle *Tribolium* exhibit sustained oscillations (Costantino & Desharnais 1991).

Noise is always present in population data and prevents oscillatory data from being exactly periodic. Any mathematical property of periodicity (phase, amplitude, average, etc.) can be affected by stochastic perturbations. In this paper, we are concerned with the relationship between stochasticity and phase. In particular, we propose one possible causal mechanism for the phenomenon of phase switching in oscillating data.

§ 2 presents time-series data illustrating the phenomenon of phase switching in a variety of contexts. § 3 uses the famous Ricker model to exemplify the mathematical theory proposed for a possible explanation of phase shifting. In § 4, we apply the theory to a multivariate map for *Tribolium* dynamics and use it to explain specific occurrences of phase switching and asynchronous replicates in laboratory cultures of *Tribolium*.

2. OBSERVED PHASE SWITCHING IN POPULATION DATA

A common phenomenon observed in oscillating laboratory cultures of *Tribolium* is a change of phase in which, for example, a high–low periodic pattern 'chicken-steps'

(skips) to a low–high pattern. Phase switching often leads to asynchronous replicates.

Phase shifts occur in many of the *Tribolium castaneum* time-series published in Desharnais & Costantino (1980). Figure 1a displays larval numbers for two of the control replicates. The cultures were shown to be oscillating with period two (Dennis *et al.* 1995). Phase shifts occur in both replicates, eventually leading to asynchrony.

A phenomenologically similar *Tribolium* example comes from an experiment conducted using a different strain in another laboratory under significantly different experimental protocols. Figure 1b plots larval numbers for two replicate time-series reported in Costantino *et al.* (1995). These cultures were also shown to be in a two-cycle regime (Dennis *et al.* 1997). One of the replicates appearing in figure 1b shifts phase, and at that particular time the replicates become asynchronous.

An example with a different animal can be seen in the data recorded by Gause (1964; tab. 3). Figure 1c presents time-series data for two replicate *Paramecium caudatum* cultures grown separately. Both replicates show two-cycle oscillations followed by several phase shifts.

A final example illustrates the phenomenon of phase switching in data cycling with period three. Three replicate time-series for *Tribolium castaneum*, as reported in Costantino *et al.* (1997), are shown in figure 1d. All three replicate cultures display three-cycle (high–low–low) behaviour, and two of the replicates shift phase. By the end of the time-series, all three replicates are oscillating out of phase.

3. THEORETICAL PHASE SWITCHING IN POPULATION MODELS

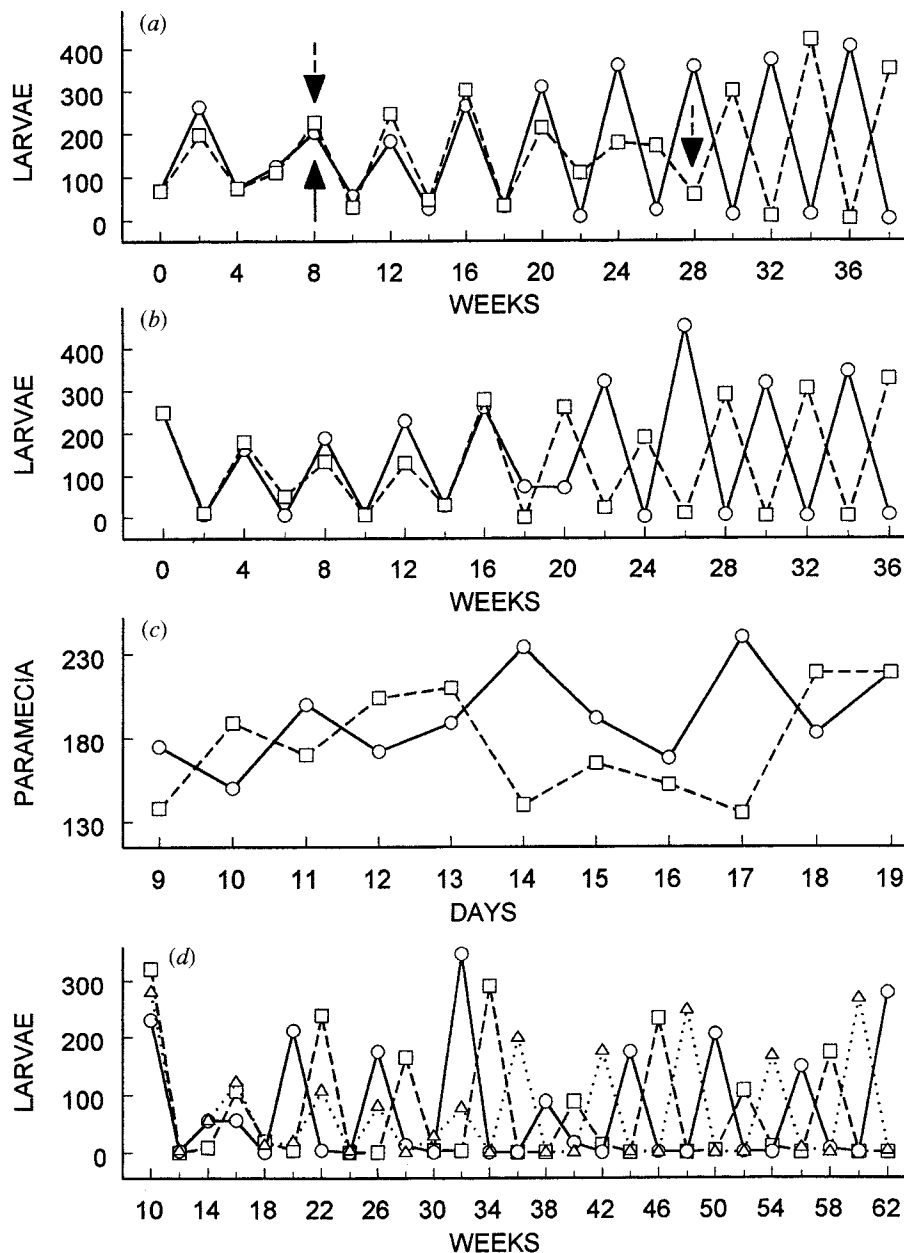In this section we use a discrete univariate map to introduce and illustrate the mathematical ideas central to

Figure 1. (*a*) *Tribolium castaneum* two-cycle data from Desharnais & Costantino (1980). Replicate A (circles) changes phase at week 8. Replicate B (squares) changes phase at weeks 8 and 28. After week 28, the replicates are asynchronous. (*b*) *Tribolium castaneum* two-cycle data from Costantino *et al.* (1995). Replicate A (squares) does not change phase. Replicate D (circles) changes phase at week 20. After week 20, the replicates are asynchronous. (*c*) *Paramecium caudatum* two-cycle data from Gause (1957). Numbers of individuals per $0.5\,cm^3$ are plotted against the number of days elapsed, with transient data (days zero to eight) omitted. Replicate no. 2 (circles) exhibits phase changes at days 14 and 16. Replicate no. 4 (squares) exhibits phase changes at days 13 and 17. (*d*) *Tribolium castaneum* three-cycle data from Costantino *et al.* (1997). Transient weeks zero to eight are omitted. All the replicates display three-cycle behaviour (high–low–low). Replicate no. 23 (squares) does not shift phase. Replicate no. 3 (circles) changes phase once, at week 16. Replicate no. 18 (triangles) changes phase at week 26, at which time it becomes synchronized with replicate no. 3. At week 36, replicate no. 18 changes phase once more. From week 36 onwards, all three replicates remain out of phase. (In fact, this situation persists until the end of the experiment, at week 80.)

our explanation of phase switching. For simplicity, we restrict our attention to cycles of period two.

The Ricker map $x_{t+1} = f(x_t)$ given by

$$x_{t+1} = bx_t e^{-cx_t},$$

is a well-known population model which generates cycles at many choices of parameters b and c. For example, when $b = 9$ and $c = 1$, the two-cycle sequence $x_0 = 1.099$, $x_1 = 3.296$, $x_2 = 1.099$, $x_3 = 3.296$, ..., is a solution (to four significant figures). Initial conditions near $x_0 = 1.099$ generate solution sequences which converge to this two-cycle; hence the two-cycle solution is labelled locally stable. The out-of-phase sequence $x_0 = 3.296$, $x_1 = 1.099$, $x_2 = 3.296$, $x_3 = 1.099$, ..., is also a locally stable two-cycle solution.

The set of points (1.099, 3.296) on the real line is an 'attractor' for the map; both of the two-cycle solutions mentioned above 'live' on this attractor. (Note that, mathematically speaking, the attractor is not a solution of the Ricker map; the attractor is just a set of two points,

not a sequence of points.) The set of initial conditions which generate solutions converging on either of the two-cycles on this attractor is denoted by B and is called the basin of attraction for the attractor. A solution starting in B will remain in B throughout time.

The basin of attraction B is composed of two noteworthy subsets: the subset B_1 of initial conditions that generate solutions converging to the first two-cycle ('up' on odd-numbered t), and the set B_2 of initial conditions that generate solutions converging to the second, out-of-phase two-cycle ('up' on even-numbered t). In this sense, each of the two-cycle solutions have their own 'basin of attraction', even though neither cycle is an 'attractor' by mathematical definition.

There is a classical way, in fact, to view the two cycles of opposite phase as separate mathematical attractors in order to bring to bear the powerful tools and concepts of a dynamical systems theory. The idea is to look at the population at every other time-step by constructing the so-called 'composite' map (e.g. see May & Oster 1976).

For the Ricker model, the population density x_{t+2} at time $t+2$ is projected from x_t by two successive applications of the Ricker map

$$x_{t+2} = f(x_{t+1}) = f(f(x_t)).$$

This is the expression we would use to calculate the population density at every second time-step. If we redefine a unit of time to be two of the original units of time, we have the composite Ricker map $x_{t+1} = f(f(x_t))$:

$$x_{t+1} = b[bx_t e^{-cx_t}]e^{-c[bx_t e^{-cx_t}]}.$$

Given an initial condition x_0, the solution sequence of the composite map corresponds to every other step of the solution sequence of the Ricker map. For example, the locally stable two-cycle solution $x_0 = 1.099$, $x_1 = 3.296$, $x_2 = 1.099$, $x_3 = 3.296$, ..., of the Ricker map corresponds to a locally stable constant solution $x_0 = 1.099$, $x_1 = 1.099$, $x_2 = 1.099$ (i.e. a locally stable fixed point $x_{e1} = 1.099$) of the composite Ricker map. Similarly, the locally stable two-cycle solution $x_0 = 3.296$, $x_1 = 1.099$, $x_2 = 3.296$, $x_3 = 1.099$, ..., of the Ricker map corresponds to a locally stable fixed point $x_{e2} = 3.296$ of the composite map. The composite Ricker map thus has two separate fixed-point attractors $\{x_{e1}\}$ and $\{x_{e2}\}$.

The set B_1 of initial conditions leading to composite map solutions which converge to the fixed-point x_{e1}, is the basin of attraction for the attractor $\{x_{e1}\}$. The basin of attraction B_2 of $\{x_{e2}\}$ is defined similarly. A solution of the composite map starting in B_1 remains in B_1 throughout time. A similar statement holds for B_2.

If, however, noise were added to the system, a solution of the composite map lying in basin B_1 might be stochastically bumped into basin B_2 at some point in time. In terms of the original Ricker map, this would correspond to a solution approaching the first two-cycle being stochastically bumped into an approach to the second (out-of-phase) two-cycle solution. If the solution was originally in phase with the first two-cycle, such a stochastic perturbation would, at least in the long run, cause a change in the phase of oscillation.

For example, consider the stochastic Ricker map

$$x_{t+1} = bx_t e^{-cx_t + \sigma E_t},$$

where E_t is a normal random variable with a mean zero and variance one (Dennis & Taper 1994). Figure 2 shows one stochastic-realization switching (composite) attractor basins and temporal phase at time $t=7$ and thereafter oscillating out of phase with the deterministic two-cycle solution.

The general concept of stochastic basin jumping is an explanation we propose for the phenomenon of phase switching in time-series data.

4. THE THEORY APPLIED TO EXPERIMENTAL DATA

In this section we apply our proposed theoretical explanation of phase switching to the control treatments (see figure 1a) reported in Desharnais & Costantino (1980). Briefly, the experimental protocol was as follows. Cultures of *Tribolium castaneum*, homozygous for the corn-oil sensitive allele (cos/cos), were initiated with 64 young adults, 15 pupae, 20 large larvae, and 70 small larvae. Each
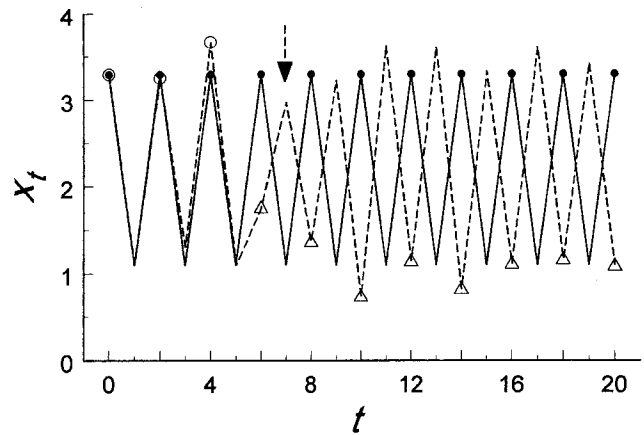

Figure 2. Ricker map time-series. Comparison of a deterministic two-cycle solution $x_0 = 3.296$, $x_1 = 1.099$, $x_2 = 3.296$, $x_3 = 1.099$, ..., (solid line) with a stochastic realization (dashed line) having variance $\sigma = 0.2$ and $x_0 = 3.296$. In both cases, $b = 9$ and $c = 1$. $x = 3.296$ is a fixed-point solution (solid circles) of the composite Ricker map, and corresponds to even time-steps of the deterministic Ricker two-cycle solution. Even time-steps of the stochastic realization are marked with open circles if they lie in the basin of attraction of the fixed-point attractor (3.296) of the composite map, and open triangles if they lie in the basin of attraction of the fixed-point attractor (1.099) of the composite map. Note the change of basin between $t=4$ and $t=6$. The phase shift in the stochastic time-series (marked by an arrow) corresponds to the jump between basins. After the phase shift, the stochastic time-series is asynchronous with the deterministic two-cycle.

population was contained in a half-pint milk bottle with 20 g of corn-oil media (90% wheat flour, 5% brewer's yeast, and 5% liquid corn oil) and kept in an unlit incubator at 33 ± 1 °C and $56\pm11\%$ relative humidity. Every two weeks all stage classes, except eggs, were censused and all stage classes, including eggs, were placed in fresh media. This procedure was followed for 38 weeks. A complete listing of the census data is given in tab. 2 in Desharnais & Liu (1987).

(a) *The LPA model*

The discrete stage-structured 'LPA' *Tribolium* model of Dennis et al. (1995) has successfully explained and predicted nonlinear phenomena in a variety of contexts, including the transitions between dynamic regimes (such as equilibria, two-cycles, three-cycles, invariant loops, and chaos), multiple attractors, and saddle influences (Costantino et al. 1995, 1997, 1998; Cushing 1996, 1998; Dennis et al. 1995, 1997; Desharnais et al. 1997; Henson et al. 1999). We now use the LPA model to explain the chicken-steps observed in Desharnais & Costantino (1980) and Dennis et al. (1995).

A stochastic version of the LPA model is given by the equations

$$L_{t+1} = bA_t \exp\left(-c_{ea}A_t - c_{el}L_t\right) \exp(E_{1t}),$$

$$P_{t+1} = L_t(1 - \mu) \exp(E_{2t}),$$

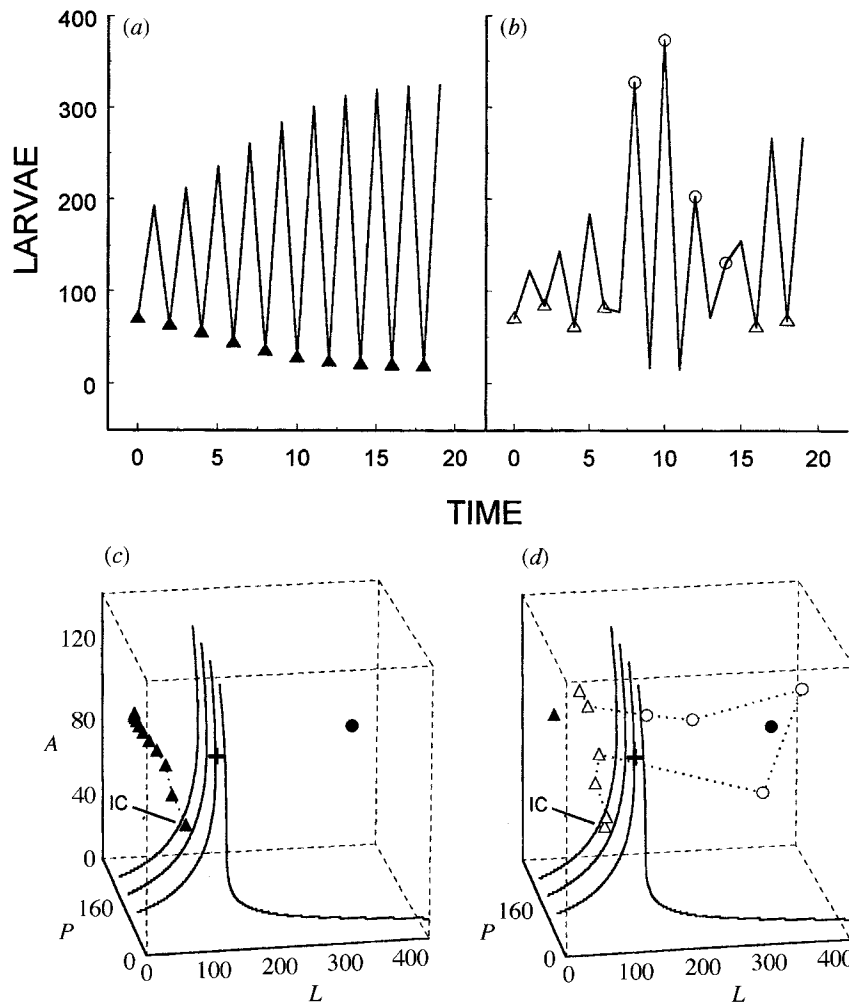$$A_{t+1} = [P_t \exp\left(-c_{pa}A_t\right) + A_t(1 - \mu_a)] \exp(E_{3t}),$$

Figure 3. LPA model predictions. (a) Deterministic model time-series with the initial condition [70, 35, 64] approaches a stable two-cycle. The composite time-series consists of the even time-steps (solid triangles). (b) A time-series realization of the stochastic LPA model with the initial condition [70, 35, 64] suffers phase shifts at $t = 7$ and $t = 15$. (c) In composite phase space, the corresponding deterministic model orbit (solid triangles) approaches the composite fixed point attractor $[L, P, A]_\triangle = [18, 158, 106]$, remaining well to the left of the basin boundary. The basin-boundary surface is indicated by cross-sections in the $P = 0, 60, 120$ and 180 planes. The cross on the boundary marks the saddle point, and the solid circle represents the composite fixed-point attractor $[L, P, A]_\bigcirc = [325, 9, 118]$. (d) In composite phase space, the stochastic time-series phase shifts appear as crossings of the basin boundary. Open triangles represent triples in the basin of $[L, P, A]_\triangle = [18, 158, 106]$; open circles represent triples in the basin of $[L, P, A]_\bigcirc = [325, 9, 118]$.

where L_t denotes the number of (feeding) larvae, P_t denotes the number of pupae (non-feeding larvae, pupae, and callow adults), and A_t denotes the number of adults. The discrete time interval is two weeks. The coefficient $b > 0$ denotes the average number of larvae recruited per adult per unit of time in the absence of cannibalism, $0 < \mu_a, \mu_l < 1$ are the adult and larval probabilities of dying from causes other than cannibalism, and the exponentials $\exp(-c_{ea}A_t - c_{el}L_t)$ and $\exp(-c_{pa}A_t)$ represent the probabilities that individuals survive cannibalism in one unit of time, with 'cannibalism coefficients' c_{el}, c_{ea}, $c_{pa} > 0$. $E_t = [E_{1t}, E_{2t}, E_{3t}]$ is a random vector assumed to have a trivariate normal distribution with mean vector zero and variance–covariance matrix Σ. $E_0, E_1, \ldots$, are assumed to be uncorrelated. We refer to the deterministic skeleton of the stochastic LPA model (obtained by setting $E_t = 0$) as the 'LPA model'. Relevant mathematical theorems concerning properties of the LPA model appear in Henson & Cushing (1997). Local stability results for both the LPA model and its composite are obtained using standard linearization techniques (Cushing 1998; Guckenheimer & Holmes 1983).

In Dennis *et al.* (1995), the maximum likely parameters estimated from the control replicates reported in Desharnais & Costantino (1980) were $b = 11.6772$, $\mu_l = 0.5129$, $c_{pa} = 0.0178$, $c_{ea} = 0.0110$, $c_{el} = 0.0093$, and $\mu_a = 0.1108$, with

$$\Sigma = \begin{pmatrix} 0.2771 & 0.0279 & 0.0098 \\ 0.0279 & 0.4284 & -0.0081 \\ 0.0098 & -0.0081 & 0.0111 \end{pmatrix}.$$

At these parameter values, the LPA model admits an unstable fixed point (rounded to the nearest beetle) of $[L, P, A] = [124, 60, 97]$.

This fixed point is stable in some directions and unstable in other directions (i.e. it is a saddle point; see Cushing *et al.* (1998)). The LPA model also predicts two locally stable two-cycle solutions: one determined by the stage vectors $[L_0, P_0, A_0] = [18, 158, 106]$, $[L_1, P_1, A_1] = [325, 9, 118]$, and the other given by the phase-shifted cycle $[L_0, P_0, A_0] = [325, 9, 118]$, $[L_1, P_1, A_1] = [18, 158, 106]$.

Because they 'live' on the same attractor ([18, 158, 106], [325, 9, 118]), the two different two-cycle solutions listed above are indistinguishable when plotted in $[L, P, A]$ space (phase space). However, these solutions do determine different phases for each component. For example, the first cycle determines a low–high oscillation in the larval component L, while the second determines a high–low oscillation in L. In order to differentiate between these out-of-phase two-cycle solutions as separate attractors with distinct basins of attraction, we turn to the composite of the LPA model.

(b) *The composite LPA model*

The 'composite LPA model' (the composite map, in which the solutions correspond to even time-steps of solutions of the LPA model) identifies the above two-cycle solutions as two different fixed point attractors given by the stage vectors $[L, P, A]_\triangle = [18, 158, 106]$, and $[L, P, A]_\bigcirc = [325, 9, 118]$.
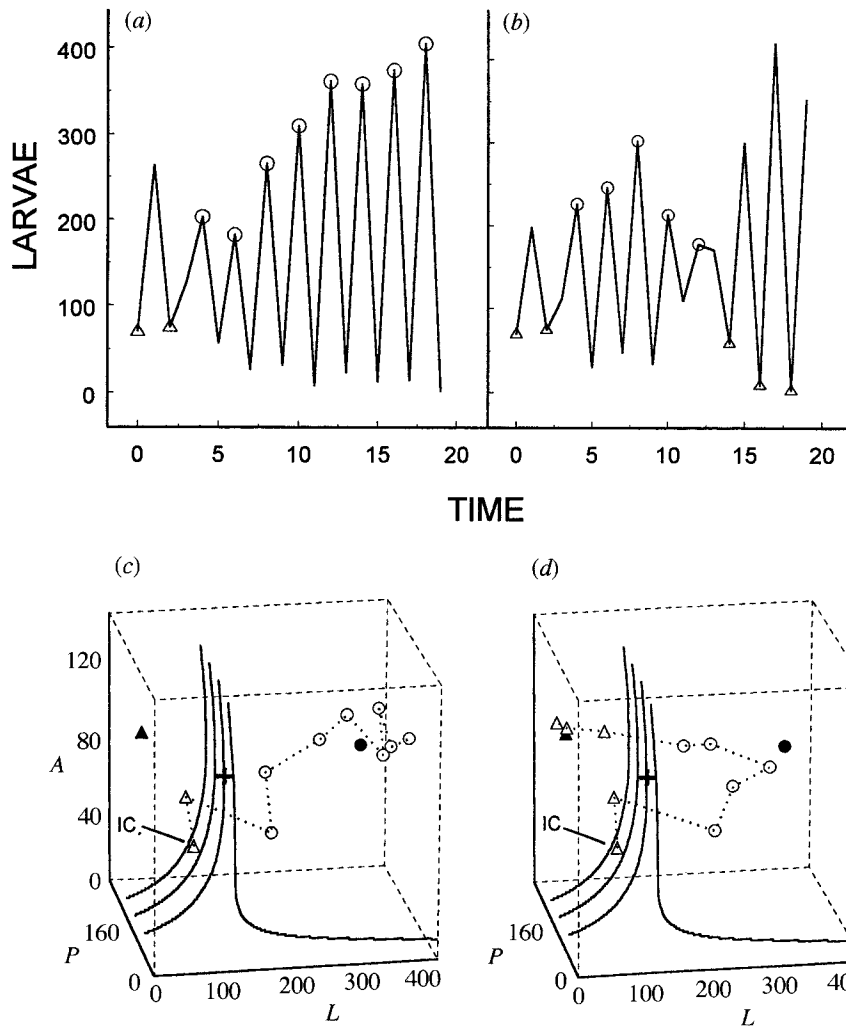
Figure 4. Data. Replicates A (*a*) and (*c*) and B (*b*) and (*d*) from Desharnais & Costantino (1980) plotted as time-series and as orbits in composite phase space using the same format as in figure 3. Open triangles represent triples in the basin of $[L, P, A]_\triangle = [18, 158, 106]$ (solid triangle); open circles represent triples in the basin of $[L, P, A]_\bigcirc = [325, 9, 118]$ (solid circle). Boundary crossings in phase space correspond to time-series phase shifts.

(Note the subscripts $\triangle$ and $\bigcirc$ are used to label the two attractors.) The saddle point of the LPA map (labelled with the subscript +) is also a saddle point $[L, P, A]_+ = [124, 60, 97]$, of the composite map.

The basins of attraction of the two stable fixed points of the composite LPA model are sets in three-dimensional phase space and are computed numerically. In this particular example, the basins are fairly simple sets. Throughout a large portion of phase space, they are separated by a two-dimensional surface (containing the saddle) which forms part of the 'basin boundary'. Initial conditions on one side of the boundary lead to composite map solutions which approach $[L, P, A]_\triangle$, while initial conditions on the other side generate composite map solutions approaching $[L, P, A]_\bigcirc$. Solutions starting on the basin boundary near the saddle point tend to the saddle $[L, P, A]_+$ (locally, the boundary is the 'stable manifold' of the unstable saddle). Indeed, near the saddle, the stable manifold of this unstable entity forms the watershed geometrical feature of phase space. Near the origin, however, the basin boundary becomes much more complicated; but this will not concern us.

(c) *Model predictions and data*

Figures 3*a* and 3*b* exhibit the larval stage time-series of both the deterministic prediction of the LPA model, and

a stochastic realization of the stochastic LPA model using the initial condition [70, 35, 64] of the experiment described above. In figures 3*c* and 3*d* appear corresponding composite phase-space plots of every other step in the time-series.

The deterministic time-series approaches the two-cycle $[L_0, P_0, A_0] = [18, 158, 106]$, $[L_1, P_1, A_1] = [325, 9, 118]$, and, in composite phase space, the corresponding solution of the composite LPA map approaches the fixed point $[L, P, A]_\triangle = [18, 158, 106]$.

The stochastic time-series, on the other hand, shifts phase at time $t=7$ and again at $t=15$. In composite phase space, the phase changes in this example occur exactly when the basin boundary is crossed.

Figure 4 presents data from the experiment using the same format as figure 3. As the LPA model predicts, *phase switching occurs in the time-series data precisely when the data cross the model predicted basin boundary in composite phase space.*

5. DISCUSSION

Populations often exhibit temporal oscillations, and sometimes these oscillations shift phase. We offer an explanation for phase shifts by means of a mix of stochastic and deterministic elements. Namely, we

hypothesize that phase shifts may correspond to stochastic jumps between basins of attraction in an appropriate phase space which associates the different phases of a periodic cycle with distinct attractors. We showed how this explanation accounts for phase shifts observed in two-cycle oscillations of *Tribolium* populations, as reported in Desharnais & Costantino (1980). In this case, phase shifts correspond exactly to stochastic jumps between the basins of attraction of two stable fixed points of the first composite of the deterministic LPA model.

More generally, for discrete autonomous models, p-cycle attractors of minimal period p admit p distinct phases, and hence correspond to p distinct (out-of-phase) attracting p-cycle solutions. Each of these p solutions corresponds to a different fixed-point attractor of the $(p-1)$-composite map (i.e. the map composed with itself $p-1$ times). If noise is added to the system, a solution of the composite map lying in a basin of attraction of one of the fixed points can be stochastically bumped into one of the other $p-1$ basins. In terms of the original map the corresponding solution, which should approach a certain p-cycle is stochastically bumped into an approach of an out-of-phase p-cycle. If the solution is originally in phase with the first cycle, such a stochastic perturbation causes (at least in the long run) a change in the phase of oscillation. The data in figure 1d provide an example of '$p=3$'-cycle phase shifting, although the basins of the second-composite map are not analyzed here.

Deterministic attractors alone do not account for the phase-switching mechanism proposed. Unstable invariant sets such as basin boundaries and saddle points, along with stochasticity, play a key role. Deterministic attractors and unstable invariant sets define, in composite phase space, the geometry that determines the behaviour of stochastic time-series.

Finally, our explanation for phase switching may be further tested by experimental investigation of new hypotheses generated by the model. For example, the frequency of phase changes should be determined by the strength of the stochasticity relative to basin sizes and shapes. Riddled or marbled basins with fractal boundaries might lead to perpetual phase shifting, disguising deterministic influences and making data fluctuations appear completely random. Even when the basins are simple, oscillations of small amplitude could contain so many phase shifts that the data would appear to be at noisy equilibrium. (This could occur, for example, because the attractors are close together in composite phase space, allowing frequent stochastic basin crossings.) On the other hand, oscillations of a large amplitude would be likely to suffer few phase shifts, depending on the size and location of the basin boundary. Specific model predictions such as these could be located in parameter space and tested in the laboratory.

REFERENCES

Costantino, R. F. & Desharnais, R. A. 1991 *Population dynamics and the* Tribolium *model*. New York: Springer.

Costantino, R. F., Cushing, J. M., Dennis, B. & Desharnais, R. A. 1995 Experimentally induced transitions in the dynamic behaviour of insect populations. *Nature* **375**, 227–230.

Costantino, R. F., Desharnais, R. A., Cushing, J. M. & Dennis, B. 1997 Chaotic dynamics in an insect population. *Science* **275**, 389–391.

Costantino, R. F., Cushing, J. M., Dennis, B., Desharnais, R. A. & Henson, S. M. 1998 Resonant population cycles in alternating habitats. *Bull. Math. Biol.* **60**, 247–273.

Cushing, J. M. 1998 *An introduction to structured population dynamics*. CBMS-NSF regional conference series in applied mathematics, vol. 71. Philadelphia: SIAM.

Cushing, J. M., Dennis, B., Desharnais, R. A. & Costantino, R. F. 1996 An interdisciplinary approach to understanding nonlinear ecological dynamics. *Ecol. Model.* **92**, 111–119.

Cushing, J. M., Dennis, B., Desharnais, R. A. & Costantino, R. F. 1998 Moving toward an unstable equilibrium: saddle nodes in population systems. *J. Anim. Ecol.* **67**, 298–306.

Dennis, B. & Taper, M. L. 1994 Density dependence in time series observations of natural populations: estimation and testing. *Ecol. Monogr.* **64**, 205–224.

Dennis, B., Desharnais, R. A., Cushing, J. M. & Costantino, R. F. 1995 Nonlinear demographic dynamics: mathematical models, statistical methods, and biological experiments. *Ecol. Monogr.* **65**, 261–281.

Dennis, B., Desharnais, R. A., Cushing, J. M. & Costantino, R. F. 1997 Transitions in population dynamics: equilibria to periodic cycles to aperiodic cycles. *J. Anim. Ecol.* **66**, 704–729.

Desharnais, R. A. & Costantino, R. F. 1980 Genetic analysis of a population of *Tribolium*. VII. Stability: response to genetic and demographic perturbations. *Can. J. Genet. Cytol.* **22**, 577–589.

Desharnais, R. A. & Liu, L. 1987 Stable demographic limit cycles in laboratory populations of *Tribolium castaneum*. *J. Anim. Ecol.* **56**, 885–906.

Desharnais, R. A., Costantino, R. F., Cushing, J. M. & Dennis, B. 1997 Estimating chaos in an insect population. *Science* **276**, 1881–1882.

Gause, G. F. 1964 *The struggle for existence*. New York: Hafner Publishing Company.

Guckenheimer, J. & Holmes, P. 1983 *Nonlinear oscillations, dynamical systems, and bifurcations of vector fields*. Berlin: Springer-Verlag.

Hassell, M. P. & May, R. M. (eds) 1990 *Population regulation and dynamics*. Cambridge University Press.

Henson, S. M. & Cushing, J. M. 1997 The effect of periodic habitat fluctuations on a nonlinear insect population model. *J. Math. Biol.* **36**, 201–226.

Henson, S. M., Costantino, R. F., Cushing, J. M., Dennis, B. & Desharnais, R. A. 1999 Multiple attractors, saddles, and population dynamics in periodic habitats. (In preparation.)

May, R. M. & Oster, G. F. 1976 Bifurcations and dynamic complexity in simple ecological models. *Am. Nat.* **110**, 573–599.

Nicholson, A. J. 1957 The self-adjustment of populations to change. *Cold Spring Harbor Symp. Quant. Biol.* **22**, 153–173.

Utida, S. 1957 Population fluctuations, an experimental and theoretical approach. *Cold Spring Harbor Symp. Quant. Biol.* **22**, 139–151.